

Development of a Compact X-ray Source and Detector System for High-Throughput, Fully Autonomous Inspection

Hidetoshi Kato,* Takeshi Fujiwara, Brian E. O'Rourke, Hiroyuki Toyokawa,
Akifumi Koike,¹ Toru Aoki,² and Ryoichi Suzuki

Research Institute for Measurement and Analytical Instrumentation (RIMA),
National Metrology Institute of Japan (NMIJ),
National Institute of Advanced Industrial Science and Technology (AIST),
Tsukuba-Central 2, 1-1-1 Umezono, Tsukuba, Ibaraki 305-8568, Japan

¹ANSeeN Inc., 3-5-1 Johoku, Hamamatsu 432-8011, Japan

²Research Institute of Electronics, Shizuoka University, 3-5-1 Johoku, Hamamatsu 432-8011, Japan

(Received September 4, 2015; accepted January 8, 2016)

Keywords: nondestructive inspection, X-ray, CdTe

We have developed a compact X-ray source using a carbon nanostructure electron emitter and an X-ray imaging camera using a CdTe semiconductor and a pixelated readout circuit for the automated X-ray inspection of metal structures such as industrial pipelines. Both the X-ray source and the detector are compact, lightweight, and battery-driven, operate with low power consumption, and generate and detect sufficiently energetic X-rays. We have also evaluated the spatial and area density resolutions by X-ray inspection test and made a comparison with commercially available products. The combination of our X-ray source and CdTe detector resulted in superior spatial and density resolutions, mainly because the detection efficiency was higher than those of the other commercially available products used in this study.

1. Introduction

To maintain the safe operation of infrastructure and industrial facilities, the demand for nondestructive testing and inspection is increasing. X-ray nondestructive testing (NDT) is one of the most promising ways of inspecting equipment in industrial facilities. However, in industrial facilities, the intended equipment for inspection is mostly complex and the space to place the X-ray source and detector is limited. Therefore, the X-ray inspection system is often required to be compact and wireless. In other words, for industrial X-ray NDT application, both the X-ray source and detector should be compact, lightweight, battery-operated, and remote-controlled, and capable of data acquisition and the generation of sufficiently intense, high-energy X-rays while minimizing the environmental dose for worker safety. To meet these demands, we are currently developing compact, cold cathode X-ray sources and X-ray cameras using a CdTe semiconductor with a pixelated readout circuit.

At the National Institute of Advanced Industrial Science and Technology (AIST), we previously developed a compact, lightweight X-ray source using a coniferous carbon nanostructure (CCNS) emitter as an electron source for nondestructive inspection.^(1,2) CCNS-based X-ray sources have no

*Corresponding author: e-mail: katou-h@aist.go.jp

warm up time and have very low power consumption. With the CCNS emitter, a current density of more than 100 mA/cm² is possible, and X-ray sources using this emitter can generate a short pulse of high-intensity X-rays. Moreover, we also demonstrated that CCNS emitters have a long lifetime even with a high emission current density.⁽³⁾

On the other hand, portable and wireless X-ray detectors for real-time imaging have become available,⁽⁴⁾ and those detectors have already been used in industrial NDT. However, the method of increasing the detection efficiency of high-energy X-rays remains to be improved. Moreover, successful developments of X-ray cameras using a CdTe element for high-energy X-ray imaging have been reported.⁽⁵⁾ The favorable characteristics of CdTe, such as high density and ability to operate at room temperature, make CdTe ideally suitable for imaging at high X-ray energies.

In this study, we evaluated spatial and area density resolutions by X-ray inspection test and made a comparison with several commercially available products.

2. X-ray Source and Detector

2.1 X-ray source

We developed an X-ray source that consists of an X-ray tube with a voltage of more than 170 kV using a CCNS emitter, a high-voltage circuit, and a drive circuit. The X-ray source has dimensions of 140 × 170 × 70 mm³ and a total weight of 2.7 kg. The X-ray tube consists of a CCNS cathode, an extraction electrode, and an anode. A negative high voltage is applied to the cathode and a positive high voltage is applied to the anode while the extraction electrode is grounded. A high voltage of ±85 kV is generated by an eight-stage Cockcroft–Walton circuit from an output AC voltage of ±8 kV (125 kHz). In the drive circuit for pulsed X-ray generation, electric power is charged to a capacitor from a battery (IDX DUO-150, output DC voltage of 14.8 V, load of 50 W, capacity of 146 Wh), then the input AC voltage of the Cockcroft–Walton circuit is generated. The diameter of the CCNS emitter is ϕ 5 mm. The focused spot of the electron beam on the X-ray target is about ϕ 1 mm in diameter. The X-ray target is tungsten and is arranged at an angle of 20 deg in the direction of X-ray emission. The X-ray window is a 5-mm-thick ceramic.

2.2 X-ray detector

We developed a pixelated CdTe X-ray camera using a direct image reading method,⁽⁵⁾ and operated it with a 5 V DC battery. The thickness of the CdTe element is 1 mm, and the pixel pitch of the readout circuit is 100 × 100 μ m². The effective size of the detector is 24 × 44 mm². After assembling with circuits and casings, the outer size and weight of the detector are 30 × 110 × 140 mm³ and 210 g, respectively.

3. Experimental Procedure

We have carried out experiments simulating the application of our X-ray NDT system to industrial pipelines.⁽⁶⁾ Schematics of the experiments to evaluate imaging capability are shown in Figs. 1(a) and 1(b). In this study, we supposed an X-ray inspection setup of a thermally insulated pipe with a metal cover [Fig. 1(c)]. The distance between the X-ray source and the detector was 200 mm, and the sample was placed right in front of the detector. An X-ray test chart (JIS Z 4916,

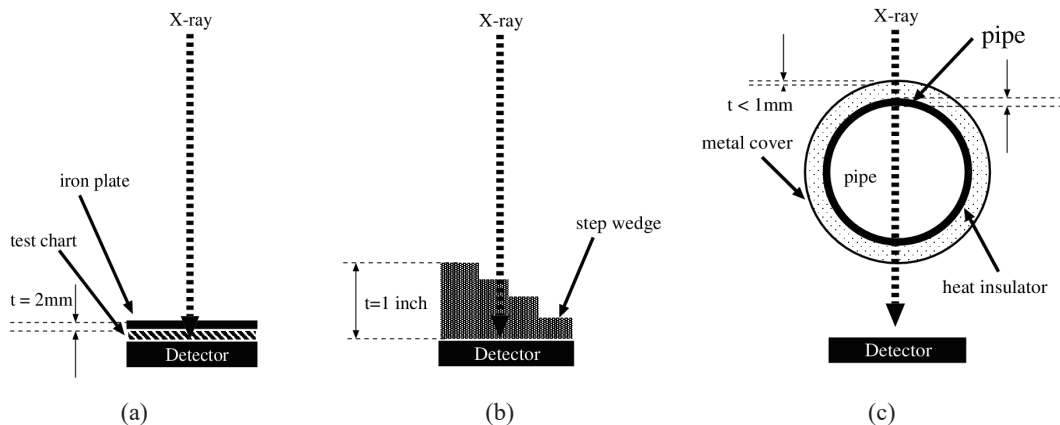


Fig. 1. Cross section of experimental setup. (a) Mock experiment for X-ray inspection over metal cover and heat insulator of pipes. 2-mm-thick iron plate + X-ray test chart for evaluation of spatial resolution. (b) Mock experiment for evaluating capability of detecting pipe wall thinning in samples of various thicknesses. Step wedge samples consisting of 1/4, 1/2, 3/4, and 1 inch stainless steel are placed in front of detectors. (c) Supposed X-ray inspection setup of pipe; the pipe is wrapped with thermal insulator and thin metal cover ($t < 1\text{ mm}$).

0.2 mm Pb) with 0.25 to 2.5 line pairs (LP)/mm was placed behind a 2-mm-thick iron plate. This plate was used to simulate the thermal insulator structure [Fig. 1(a)]. In the second experiment, a step wedge was used for the target in order to study the ability of the system to identify pipe wall thinning at various thicknesses. The wedge has four 1/4 inch steps [Fig. 1(b)]. The experimental conditions, such as X-ray intensity, experimental arrangement, and integration time, were kept constant for the comparison of detectors. The X-ray source was operated at a tube voltage of 170 kV, a tube current of 1.5 mA, and a pulse width of 50 ms in a single pulse mode. All images were taken in single shot mode (50 ms pulse), and the radiation dose at the detector was estimated to be a few hundred $\mu\text{Gy}/\text{shot}$.

For both experiments, the performance characteristics of the CdTe detector were compared with those of other commercially available detectors such as digital X-ray cameras and an imaging plate (IP). The digital X-ray cameras are NAOMI NX-06B⁽⁷⁾ from RF System Lab. and Remote RadEye 1EV⁽⁸⁾ from Teledyne DALSA Inc. The IP (FujiFilm BAS-IP MS 2040) was also used for comparison, since it is one of the widely used detectors for X-ray inspection. A summary of the properties of the detectors used is shown in Table 1.

4. Results and Discussion

Figures 2(a) and 2(b) show the radiographs and line profiles of the X-ray test chart measured through a 2-mm-thick iron plate with CdTe, RadEye, IP, and NAOMI, respectively. In Fig. 2(b), the experimental data are fitted by a Gauss function, and the fitting results are shown. We evaluated the image quality using the X-ray chart radiograph via the modulation transfer function (MTF), contrast, and noise properties. The MTF is shown in Fig. 3. On the basis of the MTF, the performance of the detectors can be ranked in the following order: RadEye > CdTe > IP > NAOMI. Because the RadEye detector has the smallest pixel size (48 μm), it showed the highest MTF value. On the other hand, the test chart number in the radiograph taken with the CdTe detector is the most

Table 1
Specifications of detectors used in this study.

	CdTe	NAOMI	RadEye	IP
Element (Thickness)	CdTe (1 mm)	Gd2O2S:Tb (NA)	Gd2O2S:Tb (NA)	BaFBr:Eu ²⁺ (NA)
X-ray detection method	Direct conversion	Scintillator + CCD camera	Scintillator + CMOS sensor	Photo-luminescence
Effective size	24 × 44 mm ²	210 × 240 mm ²	24.6 × 49.2 mm ²	200 × 400 mm ²
Pixel size	100 μm	122 μm	48 μm	100 μm
Battery operation (Voltage)	Possible (5 V DC)	Possible (12 V DC)	Possible (5 V DC)	Unable

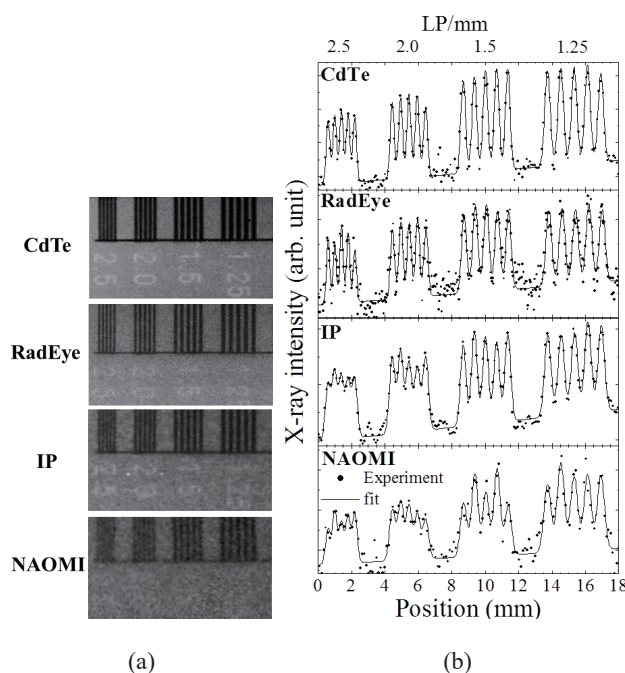


Fig. 2. (a) X-ray radiographs and (b) line profiles of the X-ray test chart taken through a 2-mm-thick iron plate (CdTe, RadEye, IP, NAOMI) for evaluation of spatial resolution.

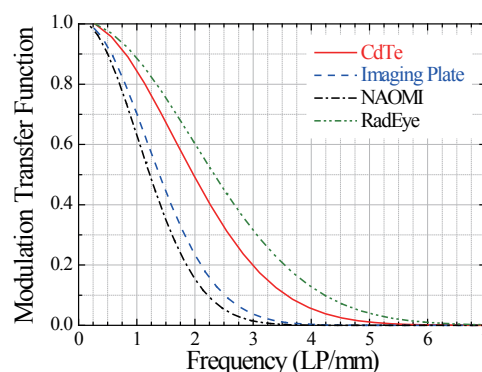


Fig. 3. (Color online) MTF of each detector obtained from the test chart line profiles.

accurate. Figure 4 shows the radiograph of part of the chart with the number “zero”. As seen in the line profiles, the highest image quality was obtained for the CdTe detector. We calculated the fluctuation of the grey level of the image to evaluate noise properties, and the detectors were ranked in the order of CdTe > RadEye > IP > NAOMI, with fluctuations of $5.7\% \pm 0.2$, $7.2\% \pm 0.2$, $7.3\% \pm 0.8$, and $8.9\% \pm 2.0$, respectively. The CdTe detector combines the highest contrast resolution and the lowest noise with good spatial resolution, and we conclude that this detector is suitable for the present study.

Figure 5 shows line profiles of the step wedge. Because X-ray radiography will be carried out for stainless-steel pipes of ~10 mm wall thickness for practical application, the density resolution should be sufficiently high to detect wall thinning of a few mm (practically ~3 mm for a 10-mm-thick pipe). From this experimental result, only the CdTe detector was able to clearly detect the

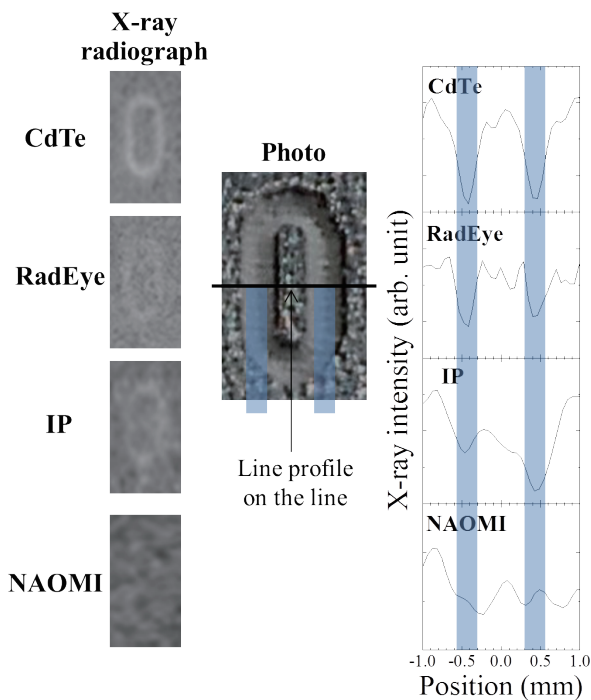


Fig. 4. (Color online) X-ray radiographs and line profiles of the number “zero” on the test chart.

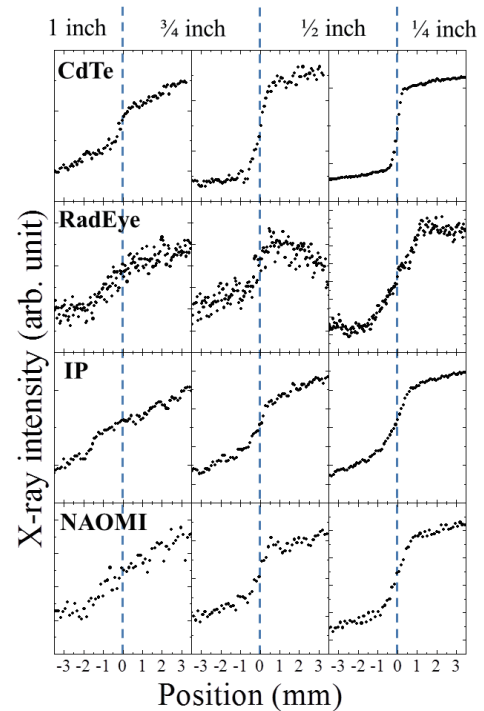


Fig. 5. (Color online) X-ray intensities obtained from the X-ray radiograph of step wedge with 4 detectors (CdTe, RadEye, IP, NAOMI).

thickness differences between 3/4- and 1-inch-thick stainless steel. It is assumed that this is because the detection efficiency of the CdTe detector is higher than those of the other detectors for high-energy X-rays penetrating thick stainless steel (3/4 inch), while other detectors are more sensitive to scattered X-rays, which reduce the image contrast. In this experiment, the energy consumed to generate an X-ray pulse is 26 J. Because the battery capacity used in the present experiment is 146 Wh, 20000 shots are generated. The small size and long lifetime of the present X-ray tube meet the major requirements for inspecting enormous lengths of pipelines using a self-propelled robot.

5. Conclusions

We developed our X-ray source and detector for the X-ray nondestructive inspection of metal structures. A compact CCNS-based pulsed X-ray source (tube voltage of 170 kV, tube current of 1.5 mA, pulse width of 50 ms, input power of 26 J) was used in combination with a 1-mm-thick 2-D CdTe detector and we compared it with several other commercially available detectors. The combination of our novel X-ray source and detector was shown to have a good MTF with 2 mm stainless steel and achieved a density resolution higher than 25% with 20 mm stainless steel. Both the source and the detector have sufficiently low power consumption; thus, the device may be completely battery-operated, and its small size and lightweight open up the possibility of X-ray nondestructive inspection in remote and confined spaces. In addition, since the device is capable of rapid imaging, the environmental dose is minimized. One possible application of the present X-ray

device is in the NDT of thinning in industrial pipelines. Increasing the X-ray energy and sensitive area of the CdTe detector will be the subject of future publications. It is also planned to mount this X-ray inspection system on a self-propelled robot and demonstrate its effectiveness in an industrial setting.

Acknowledgements

This work was supported by the New Energy and Industrial Technology Development Organization (NEDO). We are grateful to Y. Hattori, K. Asami, and I. Miura for fruitful discussions regarding pipe inspection.

References

- 1 R. Suzuki, Y. Kobayashi, and Y. Ishiguro: *Adv. X-Ray Chem. Anal. Jpn.* **41** (2010) 201 (in Japanese).
- 2 H. Kato, B. E. O'Rourke, and R. Suzuki: *JJAP Conf. Proc.* **2** (2014) 011302.
- 3 H. Kato, B. E. O'Rourke, and R. Suzuki: *Diamond Relat. Mater.* **55** (2015) 41.
- 4 General Electric: DXR250C-W/DXR250U-W Digital Detectors, <https://www.gemeasurement.com/inspection-ndt/radiography-and-computed-tomography/dxr250c-w-dxr250u-w-digital-detectors> (accessed August 2015).
- 5 T. Aoki, Y. Ishida, D. Sakashita, V. A. Gnatyuk, A. Nakamura, Y. Tomita, Y. Hatanaka, and J. Temmy: *Proc. SPIE* **5540** (2004) 196.
- 6 A. Beyer, H. Lux, and M. Wüstenbecker: Report of 10th European Conference on Non-Destructive Testing, http://www.ndt.net/article/ecndt2010/reports/1_04_26.pdf (accessed August 2015).
- 7 RF SYSTEM lab.: NAOMI-NX series, <http://industry.rfsystemlab.com/e/product/xray/nx/> (accessed August 2015).
- 8 Teledyne DALSA Inc.: X-Ray Detectors, <http://www.teledynedalsa.com/imaging/products/x-ray/> (accessed August 2015).